Academic Journal of Science and Technology
ISSN: 2771-3032 | Vol. 5, No. 2, 2023

Improving $BaTiO_3$ Energy Storage Characteristics by Doping $Bi(Mg_{2/3}Ta_{1/3})$

Dan Qie

School of Physics and Optoelectric Engineering, Guangdong University of Technology, Guangzhou Higher Education Mega Center, Guangzhou, 510006, China

Abstract: With the continuous development of modern technology, the demand for energy storage materials is also increasing. Ferroelectric energy storage materials, as a new type of material with broad application prospects, have unique advantages in storing, transmitting, and converting energy. In this work, (1-x)$BaTiO_3$-xBi($Mg_{2/3}Ta_{1/3}$)ferroelectric ceramics were synthesized in a solid-state solution. The sample of x=0.18 (0.88BT-0.12BMT) has excellent energy storage density. The excellent energy density of 3.24J/cm^3 at 260 kV/cm and the energy efficiency of 83 % at room temperature for 0.88BT-0.18BMT ceramics were achieved.

Keywords: Lead-free ferroelectrics, Bi($Mg_{2/3}Ta_{1/3}$) ceramics, $BaTiO_3$, Energy storage.

1. Introduction

With the rapid development of the times, we need materials with high energy storage to meet our needs. Currently, related equipment and products have been developed towards miniaturization, lightweight, and multi-function, which puts forward higher requirements for the density of energy storage capacitors. In general, recoverable energy storage density (W_{rec}) and energy storage efficiency (η)[1, 2]. It can be expressed by the following two Equations.

$$W_{rec} = \int_{P_r}^{P_{max}} EdP \quad (1)$$

$$\eta = \frac{W_{rec}}{W_{rec}+W_{loss}} \quad (2)$$

where W_{rec} is the recoverable energy density, P_{max} is the maximum polarization, and P_r is the remnant polarization, W_{loss} represents the unrecoverable energy density caused by the hysteresis loss. To increase energy storage, it is necessary to have a high maximum polarization value, a low residual polarization value, and a high polarization and breakdown strength. Generally, the commonly used dielectric materials in capacitors include three types of dielectric materials: linear dielectric, ferroelectric, antiferroelectric, and relaxor ferroelectric [3]. Although linear dielectric materials have high breakdown field strength and low dielectric loss, due to their own material limitations, their storage capacity is relatively low, which limits their use [4]. Ferroelectrics have higher maximum polarization values, but also higher residual polarization values and some have lower breakdown field strengths, making them unsuitable dielectric materials. Antiferroelectricity and relaxation ferroelectricity have high polarization, moderate breakdown field strength, and a low residual polarization value, which is conducive to the realization of high energy storage dielectric materials. However, antiferroelectric materials have a relatively short lifespan and most contain lead, which is not conducive to environmental protection[5, 6]. Therefore, lead-free relaxor ferroelectrics are the most promising materials for high energy storage.

2. Experimental Procedures

The usual high-temperature solid-state techniques used in this work are used to create the ceramics. By using a solid-state process, samples of (1-x)$BaTiO_3$-xBi(Mg2/3Ta1/3) ((1-x) BT-xBMT) (x=0.00, 0.18) were created. The raw powder materials used in this work are as follows, $BaCO_3$ (99.8 %), TiO_2 (99.0 %), Bi_2O_3 (99.9 %), MgO (99.9%), and Ta_2O_5 (99.99%) were batched according to their stoichiometric quantity. There is a 5% surplus increase to the amount of bismuth oxide because the loss of bismuth in high temperature conditions is taken into account. Finally, using a planetary ball mill, yttrium stabilized zirconia balls and anhydrous ethanol are combined for 24 hours in a polyethylene tank. The next steps involve drying and screening. The powder is then heated to between 900 and 1100 degrees Celsius in an alumina crucible for three hours to produce a single perovskite phase. Hence, in order to learn more The calcined powder was mixed with yttrium stabilized zirconia balls and anhydrous ethanol as the medium for grinding for 12 hours in a polyethylene tank to achieve good homogeneity. It is then dried and sieved one more. Following the creation of particles from these thoroughly combined powders using a PVB adhesive, a hydraulic press is used to crush the particles into a disc with an 11 millimeter diameter and a thickness of roughly 1 millimeter. To lessen experimental mistakes brought on by bismuth evaporation, bury calcined powder of the same composition under the plate in a covered crucible. To create a bulk ceramic sheet, these samples were then further sintered for three hours between 1150 and 1300 °C.

To describe the crystal structure, X-ray diffraction (XRD, D8 ADVANCE, Bruker, Germany) was employed. Ceramics' microstructure as seen through a field-emission scanning electron microscope (FESEM, SU8220, Hitachi, Japan). The microstructure of ceramics was studied using field emission scanning electron microscopy (FE-SEM).

3. Results and Discussion

3.1. Phase and structure analyses

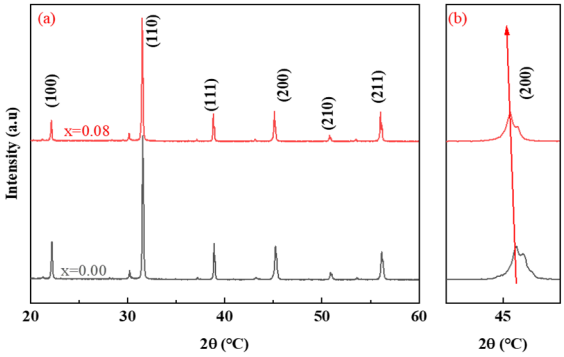

Figure 1. (a) XRD patterns for (1-x)BT-xBMT ceramics at room temperature.
(b) The amplified diffraction peak of (1-x)BT-xBMT ceramics range from 44-46 °C.

Fig. 1 shows the X-ray diffraction (XRD) spectra for sintered (1-x)BT-xBMT ceramics at room temperature. All the ceramics exhibit a single perovskite phase with no detectable impurity. This suggests that the BMT can enter the BT matrix. This means that the ions have all been dissolved in the BT lattices. With the gradual increase of x, the (200) peak gradually moved to a lower angle, indicating that the cell volume expanded. Fig. 1(b) shows that doping leads to the symmetry transition of crystal structure, from the tetragonal phase to the pseudocubic phase. When the value range of x is 0.00~0.21, The weak (002) peak gradually moves to the (200) peak, and the (002)/(200) peak is merged into one (200) peak [7]. The reason for this may be the lattice expansion due to the different ionic radii at the B-site. The lattice expansion may be due to the substitution of Mg^{2+}(0.72 Å) and Ta^{5+}(0.69 Å) cations for the Ti^{4+}(0.605 Å).

3.2. Morphology and chemical analyses

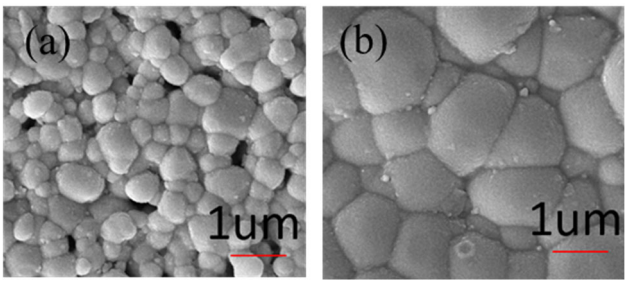

Figure 2. SEM micrographs with insets showing the grain size distributions of (1-*x*)BT-*x*BMT ceramics: (a) *x*=0.00, (b) *x*=0.18

The SEM images of (1-x) BT-xBMT ceramics are shown in FIG. 2 (a) and (b). It can be clearly seen that when there is no doping, although the grain size is small, there are many hole defects. When x=0.18, although the grain size is increased, the hole defects are significantly reduced. This may lead to enhanced energy storage performance

3.3. P-E hysteresis loops and energy storage capability

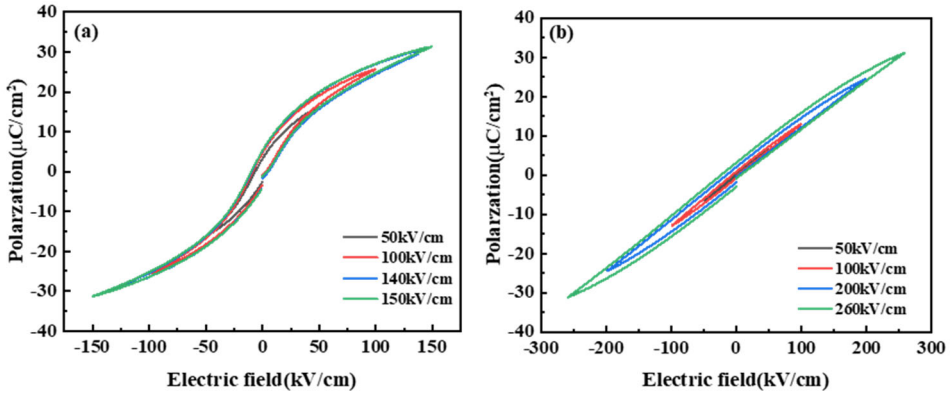

Figure 3. The P-E hysteresis loops. (a)x=0.00 (b) x=0.18

When undoped,for pure $BaTiO_3$, it can be calculated from FIG. 3. (a) when the electric field strength is 150 kv/cm. The calculated energy storage is 1.34J/cm^3, with an efficiency of 73.24%. When doped with BMT,for x=0.18, it can be calculated from FIG. 3. (b) that the energy storage is 3.24 J/cm^3, and the efficiency is 83.19 %.

4. Summary

A new type of lead-free (1-x) BT-xBMT ceramic was prepared by conventional solid-state method. By doping $BaTiO_3$ with BMT, the energy storage and small efficiency of $BaTiO_3$ have been significantly increased. Through BMT modification, the grain pores of BT-BMT ceramics are significantly reduced, which is beneficial to improving the dielectric breakdown strength. By calculating the ferroelectric energy storage and efficiency, it is found that the energy storage reaches 3.24 J/cm^3 and the efficiency is 83.19 %. These advantages make bt-based relaxor ferroelectric ceramics have great application potential in high-power pulse capacitors.

References

[1] L. Wang, P.L. Patel, S. Yu, B. Liu, J. McLeod, L.E. Clarke, W. Chen, Win–Win strategies to promote air pollutant control policies and non-fossil energy target regulation in China, Applied Energy 163 (2016) 244-253.

[2] R. Lamedica, E. Santini, A. Ruvio, L. Palagi, I. Rossetta, A MILP methodology to optimize sizing of PV - Wind renewable energy systems, Energy 165 (2018) 385-398.

[3] L. Wang, Y. Bai, X. Lu, J.L. Cao, L.J. Qiao, Ultra-low percolation threshold in ferrite-metal cofired ceramics brings

both high permeability and high permittivity, Sci Rep 5 (2015) 7580.

[4] M. Rabuffi, G. Picci, Status quo and future prospects for metallized polypropylene energy storage capacitors, IEEE Transactions on Plasma Science 30(5) (2002) 1939-1942.

[5] P. Qiao, Y. Zhang, X. Chen, M. Zhou, G. Wang, X. Dong, Effect of Mn-doping on dielectric and energy storage properties of (Pb0.91La0.06) (Zr0.96Ti0.04)O3 antiferroelectric ceramics, Journal of Alloys and Compounds 780 (2019) 581-587.

[6] J. Shen, X. Wang, T. Yang, H. Wang, J. Wei, High discharge energy density and fast release speed of (Pb, La)(Zr, Sn, Ti)O3 antiferroelectric ceramics for pulsed capacitors, Journal of Alloys and Compounds 721 (2017) 191-198.

[7] X. Chen, X. Li, J. Sun, C. Sun, J. Shi, F. Pang, H. Zhou, Achieving ultrahigh energy storage density and energy efficiency simultaneously in barium titanate based ceramics, Applied Physics A 126(2) (2020).